The Canadian Mineralogist
Vol. 57, pp. 457-466 (2019)
DOI: 10.3749/canmin.1800067

MEIERANITE, $Na_2Sr_3MgSi_6O_{17}$, A NEW MINERAL FROM THE WESSELS MINE, KALAHARI MANGANESE FIELDS, SOUTH AFRICA

HEXIONG YANG§

Department of Geosciences, University of Arizona, 1040 E. 4th Street, Tucson, Arizona 85721-0077, USA

XIANGPING GU

School of Geosciences and Info-Physics, Central South University, Changsha, Hunan 410083, China

ROBERT T. DOWNS AND STANLEY H. EVANS

Department of Geosciences, University of Arizona, 1040 E. 4th Street, Tucson, Arizona 85721-0077, USA

JACO J. VAN NIEUWENHUIZEN

Plot 968, Alheit, Kakamas 8870, Northern Cape, South Africa

ROBERT M. LAVINSKY

P.O. BOX 830460, Richardson, Texas 75083, USA

XIANDE XIE

Key Laboratory of Mineralogy and Metallogeny, Guangzhou Institute of Geochemistry, CAS, and Guangdong Key Laboratory of Mineral Physics and Materials, Guangzhou 510640, China

ABSTRACT

A new mineral species, meieranite, ideally $Na_2Sr_3MgSi_6O_{17}$, has been found in the Wessels mine, Kalahari Manganese Fields, Northern Cape Province, South Africa. It occurs in isolated aggregates embedded in a matrix mainly of sugilite, along with minor aegirine and pectolite. Crystals of meieranite are up to $0.5 \times 0.5 \times 0.4$ mm in size. No twinning is observed. The mineral is light blue to blue in transmitted and under incident lights, transparent with white streak, and has vitreous luster. It is brittle and has a Mohs hardness of 5.5; cleavage is good on {010} and no parting was observed. The measured and calculated densities are 3.41(3) and 3.410 g/cm^3, respectively. Optically, meieranite is biaxial (–), with $\alpha = 1.610(1)$, $\beta = 1.623(1)$, $\gamma = 1.630(1)$ (white light), 2V (meas.) = 70(1)°, 2V (calc.) = 72°. The calculated compatibility index based on the empirical formula is –0.007 (superior). An electron microprobe analysis yields an empirical formula (based on 17 O *apfu*) of $Na_{1.96}(Sr_{2.91}Ba_{0.03}Ca_{0.03}Pb_{0.02})_{\Sigma 2.99}(Mg_{0.62}Mn_{0.28}Co_{0.07}Fe_{0.01})_{\Sigma 0.98}Si_{6.03}O_{17}$, which can be simplified to $Na_2Sr_3MgSi_6O_{17}$.

Meieranite is orthorhombic, with space group $P2_1nb$ and unit-cell parameters a 7.9380(2), b 10.4923(3), c 18.2560(6) Å, and V 1520.50(8) Å^3. Its crystal structure is characterized by two kinds of layers that alternate along [010]: layers of corner-sharing SiO_4 and $M^{2+}O_4$ tetrahedra (M^{2+} = Mg, Mn, Co, Fe) and layers of NaO_6 and SrO_8 polyhedra. The tetrahedral layers consist of eight-, five-, and four-membered rings and are composed of $[Si_6O_{17}]$ ribbons (parallel to [101]) linked together by MO_4 tetrahedra. Most remarkably, the structure of meieranite is topologically identical to that of the nordite group of minerals, which has the general chemical formula $Na_3SrR^{3+}M^{2+}Si_6O_{17}$, where R = Ce and La and M = Zn, Fe, and Mn. Accordingly, chemically, meieranite may be obtained through the coupled substitution of $2Sr^{2+}$ for $(Na^+ + R^{3+})$ in nordite.

Keywords: meieranite, nordite, crystal structure, X-ray diffraction, Raman spectra.

§ *Corresponding author e-mail address*: hyang@email.arizona.edu

Introduction

A new mineral species, meieranite, ideally $Na_2Sr_3MgSi_6O_{17}$, has been found in the Wessels mine, Kalahari Manganese Fields, Northern Cape Province, Republic of South Africa. It is named in honor of Dr. Eugene Stuart Meieran, a member of the U.S. National Academy of Engineering. Gene received his M.S. and Sc.D. in Materials Science from the Massachusetts Institute of Technology in 1963. Since then, he has worked on many of the important problems that impacted the emerging semiconductor industry, including purification, analyses, and quality control for the raw materials required for modern microchips. Gene joined Intel Corp. in 1973 and was named Fellow in 1984 and Senior Intel Fellow in 2003. He has approximately 60 technical publications, of which 20 are about X-ray topographic studies of defects in nearly perfect semiconductor crystals. He is also an advocate of education and was responsible for the Intel International Science and Engineering Fair (IISEF), helping to expand and promote scientific literacy in youths. Gene started collecting minerals in 1949, with his present specialization in high-quality gem species and native silver. In addition to his time serving on boards of several mineral museums, Gene has donated a number of important specimens to major museums, including Harvard, the Smithsonian, University of Arizona, Rice, and Yale. For his work in mineral preservation and education, he was awarded the prestigious Carnegie Medal in 2004 by The Carnegie Museum. Gene is a co-founder of the science session at the Dallas Mineral Collectors Symposium. Recently, he helped found a new mineral museum in Los Angeles, California. The new mineral and its name have been approved by the Commission on New

TABLE 1. ELECTRON MICROPROBE ANALYSIS DATA FOR MEIERANITE

Constituent	wt.%	Range	Stand. Dev.	Probe Standard
SiO_2	46.16	45.52–46.74	0.42	SiO_2
CaO	0.21	0.18–0.25	0.03	$CaMgSi_2O_6$
MgO	3.21	2.74–4.29	0.53	MgO
MnO	2.53	1.59–3.52	0.64	$MnSiO_3$
FeO	0.10	0.00–0.26	0.08	Fe_2SiO_4
Na_2O	7.75	7.52–8.11	0.17	$NaAlSi_3O_8$
SrO	38.39	38.07–38.97	0.26	$SrSO_4$
BaO	0.52	0.25–0.90	0.23	$BaSO_4$
CoO	0.69	0.41–0.81	0.13	CoO
PbO	0.56	0.23–0.83	0.23	$Pb_5(VO_4)_3Cl$
Total	100.12	99.46–100.62	0.47	

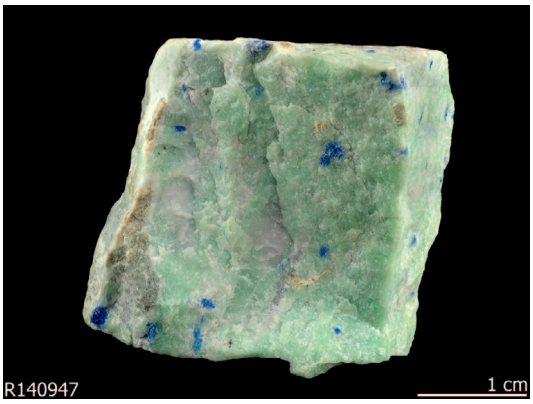

FIG. 1. Rock samples on which aggregates of granular blue meieranite crystals are found. Associated minerals are massive pale green sugilite, prismatic grey aegirine, and bladed white pectolite.

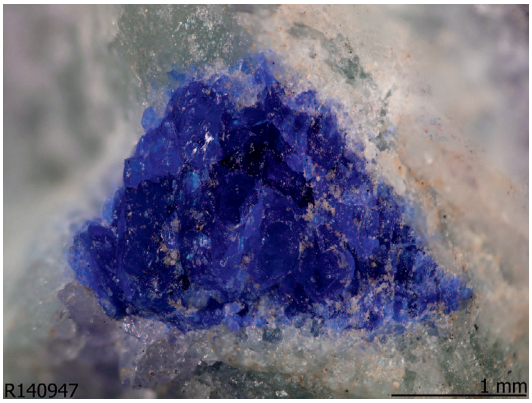

FIG. 2. A microscopic view of meieranite, associated with pale green sugilite.

TABLE 2. POWDER X-RAY DIFFRACTION DATA FOR MEIERANITE

I_{meas} %	I_{cal} %	d_{meas}	d_{calc}	*h*	*k*	*l*
3.6	12.0	7.276	7.276	1	0	1
6.4	14.6	4.828	4.826	1	0	3
3.4	2.2	4.547	4.541	0	2	2
15.4	22.2	4.253	4.250	1	2	1
5.1	3.8	3.962	3.967	2	0	0
25.1	**41.6**	**3.550**	**3.549**	**1**	**2**	**3**
11.3	16.7	3.436	3.439	0	2	4
42	**33.3**	**3.166**	**3.162**	**2**	**2**	**0**
100	**100.0**	**2.990**	**2.988**	**2**	**2**	**2**
83.9	**98.1**	**2.800**	**2.801**	**1**	**2**	**5**
26.4	**15.2**	**2.623**	**2.619**	**0**	**4**	**0**
9.9	16.2	2.474	2.475	1	0	7
17.2	25.6	2.425	2.425	3	0	3
9.2	8.4	2.391	2.389	2	2	5
7	5.7	2.361	2.361	3	2	0
5.3	2.4	2.341	2.341	3	2	1
4.5	3.5	2.306	2.302	1	4	3
3.2	0.1	2.287	2.280	0	0	8
5.6	5.6	2.201	2.201	3	2	3
21.2	15.4	2.126	2.125	2	4	2
4.2	0.3	2.091	2.088	0	3	7
27.1	**23.7**	**2.057**	**2.055**	**1**	**4**	**5**
13.5	4.9	1.982	1.984	4	0	0
5.9	6.2	1.937	1.938	4	0	2
17.8	14.7	1.853	1.856	3	0	7
14.7	7.9	1.818	1.819	4	0	4
8.4	14.8	1.798	1.799	1	4	7
24.8	**25.0**	**1.778**	**1.779**	**3**	**4**	**3**
17.8	12.6	1.749	1.749	3	2	7
4.6	6.3	1.721	1.722	0	2	10
5.4	1.8	1.677	1.676	1	6	2
5.3	7.4	1.657	1.657	2	0	10
2.5	1.9	1.597	1.598	2	6	0
15.1	11.0	1.575	1.574	2	6	2
13.6	12.2	1.546	1.545	1	6	5
9.6	5.2	1.514	1.513	5	2	1
4.7	4.2	1.494	1.494	4	4	4
4.2	3.2	1.439	1.439	4	2	8
12.4	11.8	1.400	1.402	5	2	5
7	10.2	1.368	1.370	2	2	12
3.7	1.3	1.354	1.355	5	0	7
4.5	5.7	1.340	1.343	4	0	10
5.5	4.5	1.307	1.308	2	6	8
5	5.0	1.299	1.297	4	6	2
6.6	4.3	1.270	1.272	3	6	7
3	3.4	1.248	1.248	2	4	12
4.1	1.1	1.233	1.232	2	8	2
2.6	2.5	1.214	1.215	5	2	9
3.4	1.4	1.204	1.206	3	2	13
4	2.7	1.181	1.180	6	4	0
3.7	4.0	1.172	1.171	1	2	15
3.9	4.0	1.159	1.157	1	8	7
4.4	5.5	1.154	1.152	3	8	3

Minerals, Nomenclature and Classification (CNMNC) of the International Mineralogical Association (IMA 2015-009). The cotype samples have been deposited at the University of Arizona Mineral Museum (Catalogue # 20011) and the RRUFF Project (deposition # R140947).

This paper describes the physical and chemical properties of meieranite and its crystal structure determined from single-crystal X-ray diffraction data, demonstrating that the structure of meieranite exhibits all principal features of the nordite structural type.

Sample Description and Experimental Methods

Occurrence, physical and chemical properties, and Raman spectra

The type sample of meieranite was found on a specimen collected from the Wessels mine, Kalahari Manganese Fields, Northern Cape Province, Republic of South Africa (27°6′51.82″S, 22°51′18.31″E). It occurs in isolated aggregates embedded in a matrix consisting of mainly pale-green sugilite, along with minor prismatic grey aegirine and colorless pectolite (Figs. 1 and 2). The mineral assemblage probably formed as a result of a hydrothermal event. Conditions during metamorphism were in the range of 270–420 °C at 0.2–1.0 kbar (Kleyenstuber 1984, Gutzmer & Beukes 1996). Detailed reviews of the geology and mineralogy of the Kalahari Manganese Fields have been given by Kleyenstuber (1984), Von Bezing *et al*. (1991), and Gutzmer & Beukes (1996).

Meieranite crystals in aggregates are granular, up to 0.5 × 0.5 × 0.4 mm in size. No twinning is observed macroscopically. The mineral is light blue to blue, transparent with pale blue streak, and has vitreous luster. It is brittle and has a Mohs hardness of 5.5; cleavage is good on {010} and no parting was observed. The measured and calculated densities are 3.41(3) and 3.410 g/cm^3, respectively. Optically, meieranite is biaxial (–), with $\alpha = 1.610(1)$, $\beta = 1.623(1)$, $\gamma = 1.630(1)$ (white light), 2V (meas.) = 70(1)°, 2V (calc.) = 72°, and the orientation $X = a$, $Y = b$, $Z = c$, with X = violet, Y = blue/violet, and Z = blue. The pleochroism is strong dark blue to violet and the dispersion is strong with r > v. The calculated compatibility index based on the empirical formula is –0.007 (superior) (Mandarino 1981). Meieranite is insoluble in water, acetone, and hydrochloric acid.

The chemical composition was determined using a Shimadzu EPMA-1720 electron microprobe (WDS mode, 15 kV, 10 nA, and a beam diameter of 1 μm). The standards used are listed in Table 1, along with the determined compositions (nine analysis points). The resultant chemical formula, calculated on the basis of 17 O atoms *pfu* (from the structure determination), is

TABLE 3. COMPARISON OF MINERALOGICAL DATA FOR NORDITE-GROUP MINERALS AND MEIERANITE

	Nordite-(La)	Ferronordite-(Ce)	Manganonordite-(Ce)	Meieranite
Ideal chemical formula	$Na_3SrLaZnSi_6O_{17}$	$Na_3SrCeFe^{2+}Si_6O_{17}$	$Na_3SrCeMn^{2+}Si_6O_{17}$	$Na_2Sr_3MgSi_6O_{17}$
Crystal symmetry	Orthorhombic	Orthorhombic	Orthorhombic	Orthorhombic
Space group	*Pcca*	*Pcca*	*Pcca*	$P2_1nb$
a (Å)	14.27(3)	14.46(1)	14.44(2)	7.9380(2)
b (Å)	5.16(1)	5.194(3)	5.187(5)	10.4923(3)
c (Å)	19.45(15)	19.874(9)	19.82(1)	18.2560(6)
V (Å^3)	1432.2	1492.39	1485.10	1520.50(8)
Z	4	4	4	4
ρ_{cal} (g/cm^3)	3.48			3.44
2θ range for data collection		≤100.26	≤102.84	≤64.86
No. of reflections collected		4016	5265	12218
No. of independent reflections		3803	3534	5296
No. of reflections with $I > 2\sigma(I)$	1335	3623	3433	4738
No. of parameters refined				265
R(int)				0.023
Final R_1, wR_2 factors [$I > 2\sigma(I)$]	0.122	0.054	0.044	0.027, 0.063
Goodness-of-fit				1.034
Reference	(1)	(2)	(2)	(3)

References: (1) Bakakin *et al.* (1970); (2) Pushcharovskii *et al.* (1999); (3) this study.

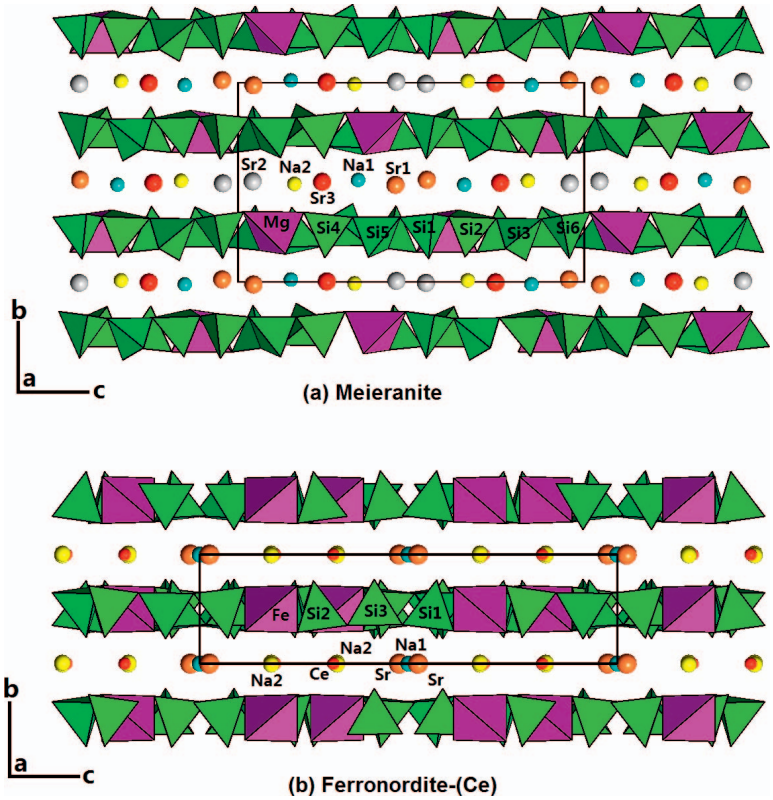

FIG. 3. Crystal structures of (a) meieranite and (b) ferronordite-(Ce), viewed along the **a** axis. Purple and yellow tetrahedra represent SiO_4 and $M^{2+}O_4$ groups (M^{2+} = Mg, Mn, Co, Fe, Zn), respectively. Green, brown, and red spheres represent Na^+, Sr^{2+}, and R^{3+} (= Ce and La).

TABLE 4. ATOMIC COORDINATES AND DISPLACEMENT PARAMETERS FOR MEIERANITE

Atom	*x*	*y*	*z*	U_{eq}	U_{11}	U_{22}	U_{33}	U_{23}	U_{13}	U_{12}
Na1	0.1912(3)	0.0118(2)	0.1530(1)	0.0202(5)	0.0335(13)	0.0129(11)	0.0142(10)	0.0036(8)	0.0081(10)	0.0052(9)
Na2	0.2113(3)	0.4923(2)	0.1632(1)	0.0230(6)	0.0377(15)	0.0132(11)	0.0181(10)	–0.0045(8)	0.0144(10)	–0.0079(10)
Sr1	0.07821(6)	0.51278(4)	0.54523(2)	0.0086(1)	0.0103(2)	0.0084(2)	0.0070(2)	0.0015(1)	0.0016(2)	0.0007(3)
Sr2	0.07794(6)	0.49507(4)	0.95728(2)	0.0069(1)	0.0077(2)	0.0069(2)	0.0062(2)	0.0003(1)	0.0000(2)	0.0003(2)
Sr3	0.26764(6)	0.49756(4)	0.75671(2)	0.0067(1)	0.0074(2)	0.0061(2)	0.0075(2)	–0.0012(1)	–0.0003(2)	0.0001(2)
M	0.4083(1)	0.7446(1)	0.89559(6)	0.0045(2)	0.0040(5)	0.0074(5)	0.0022(4)	0.0011(4)	0.0002(3)	–0.0004(4)
Si1	0.2746(2)	0.7336(1)	0.45098(6)	0.0052(2)	0.0067(6)	0.0038(6)	0.0050(5)	–0.0003(4)	0.0003(5)	0.0000(5)
Si2	0.0646(2)	0.2752(1)	0.66099(6)	0.0082(2)	0.0111(6)	0.0075(6)	0.0060(5)	–0.0003(4)	–0.0004(5)	0.0006(6)
Si3	–0.0621(2)	0.7222(1)	0.69269(7)	0.0077(2)	0.0092(5)	0.0069(6)	0.0070(5)	–0.0005(4)	–0.0007(5)	–0.0001(5)
Si4	0.5687(2)	0.7291(1)	0.74253(6)	0.0068(3)	0.0071(6)	0.0048(6)	0.0083(5)	0.0003(4)	0.0005(6)	0.0000(6)
Si5	0.4044(2)	0.2695(1)	0.89949(7)	0.0059(2)	0.0054(6)	0.0082(6)	0.0041(5)	0.0005(5)	0.0007(4)	–0.0001(5)
Si6	0.2702(2)	0.2307(1)	0.44859(6)	0.0050(2)	0.0065(5)	0.0040(6)	0.0046(5)	0.0001(4)	0.0007(5)	0.0003(5)
O1	0.3387(5)	0.6757(3)	0.5322(2)	0.0101(7)	0.0135(16)	0.0087(17)	0.0082(15)	0.0032(13)	–0.0029(12)	–0.0006(13)
O2	0.2727(6)	0.3834(3)	0.0504(2)	0.0099(6)	0.0132(17)	0.0068(16)	0.0097(13)	0.0016(12)	–0.0024(15)	0.0007(15)
O3	0.1006(4)	0.6592(3)	0.4362(2)	0.0092(6)	0.0091(16)	0.0091(15)	0.0093(14)	–0.0008(11)	–0.0003(13)	–0.0013(12)
O4	0.4105(5)	0.6718(3)	0.3920(2)	0.0106(6)	0.0125(16)	0.0067(14)	0.0125(15)	–0.0022(13)	0.0079(13)	–0.0025(14)
O5	0.2266(5)	0.3601(3)	0.6376(2)	0.0102(7)	0.0093(16)	0.0092(17)	0.0120(15)	–0.0002(13)	0.0001(12)	0.0012(12)
O6	0.0881(6)	0.1258(3)	0.6554(2)	0.0156(7)	0.0266(20)	0.0105(17)	0.0097(14)	–0.0029(12)	–0.0054(17)	0.0067(18)
O7	0.0172(5)	0.8194(3)	0.7540(2)	0.0067(7)	0.0122(17)	0.0046(17)	0.0034(13)	–0.0002(11)	–0.0028(12)	–0.0010(13)
O8	0.0556(5)	0.6081(3)	0.6687(2)	0.0113(7)	0.0139(19)	0.0099(16)	0.0101(14)	–0.0026(12)	–0.0003(14)	0.0059(14)
O9	–0.2398(5)	0.6686(3)	0.7282(2)	0.0110(6)	0.0102(15)	0.0084(15)	0.0143(15)	0.0011(12)	0.0010(15)	–0.0012(14)
O10	0.3838(4)	0.1837(3)	0.3761(2)	0.0091(7)	0.0131(16)	0.0075(16)	0.0068(14)	0.0010(12)	0.0053(12)	–0.0001(13)
O11	0.4892(5)	0.6499(3)	0.8096(2)	0.0104(7)	0.0130(16)	0.0088(16)	0.0093(15)	0.0032(12)	0.0007(13)	–0.0029(13)
O12	0.5656(6)	0.3791(3)	0.7509(2)	0.0095(7)	0.0108(19)	0.0082(18)	0.0095(14)	0.0004(10)	0.0020(13)	–0.0006(17)
O13	0.4634(5)	0.6755(3)	0.6686(2)	0.0094(7)	0.0117(16)	0.0084(16)	0.0080(15)	–0.0007(12)	0.0000(13)	–0.0033(12)
O14	0.2739(5)	0.3758(3)	0.8768(2)	0.0126(7)	0.0144(17)	0.0118(17)	0.0115(14)	0.0027(13)	0.0037(15)	0.0065(16)
O15	0.0820(5)	0.6676(3)	0.0671(2)	0.0084(6)	0.0061(13)	0.0075(14)	0.0115(14)	–0.0007(11)	0.0020(15)	0.0002(15)
O16	0.2702(6)	0.3811(3)	0.4562(2)	0.0104(7)	0.0136(17)	0.0065(16)	0.0111(14)	0.0002(12)	0.0016(16)	0.0006(15)
O17	0.3403(4)	0.6487(3)	0.9842(2)	0.0085(6)	0.0094(15)	0.0086(16)	0.0076(14)	–0.0029(12)	–0.0004(13)	0.0003(13)

Note: During the structure refinement, the trace amounts of Fe and Co were treated as Mn. Therefore, the *M* site is occupied by (0.63Mg + 0.37Mn).

TABLE 5. SELECTED BOND DISTANCES IN MEIERANITE

	Distance (Å)		Distance (Å)
Na1–O12	2.345(3)	M–O11	1.966(2)
–O3	2.359(3)	–O3	1.975(3)
–O9	2.401(3)	–O5	1.979(2)
–O16	2.500(3)	–O17	1.981(2)
–O4	2.554(3)	Ave.	1.975
–O13	2.685(3)		
Ave.	2.474	Si1–O2	1.572(2)
		–O3	1.609(3)
Na2–O12	2.370(3)	–O4	1.657(3)
–O11	2.362(3)	–O1	1.682(2)
–O2	2.406(3)	Ave.	1.630
–O10	2.535(3)		
–O9	2.631(3)	Si2–O6	1.582(2)
–O15	2.743(3)	–O5	1.622(3)
Ave.	2.508	–O4	1.655(3)
		–O7	1.663(2)
Sr1–O8	2.473(2)	Ave.	1.631
–O3	2.520(2)		
–O5	2.608(2)	Si3–O8	1.580(2)
–O4	2.615(2)	–O7	1.640(2)
–O16	2.622(2)	–O9	1.652(3)
–O16	2.687(3)	–O10	1.655(2)
–O1	2.693(3)	Ave.	1.631
–O1	3.086(3)		
Ave.	2.663	Si4–O12	1.579(2)
		–O11	1.609(2)
Sr2–O6	2.474(2)	–O9	1.667(3)
–O14	2.479(2)	–O13	1.684(2)
–O2	2.579(2)	Ave.	1.635
–O17	2.641(2)		
–O17	2.679(2)	Si5–O14	1.577(3)
–O15	2.701(2)	–O13	1.655(2)
–O2	2.742(3)	–O1	1.672(2)
–O10	2.844(2)	–O15	1.672(3)
Ave.	2.642	Ave.	1.644
Sr3–O6	2.532(2)	Si6–O16	1.584(2)
–O14	2.538(2)	–O17	1.598(2)
–O11	2.565(2)	–O15	1.659(3)
–O8	2.600(2)	–O10	1.675(2)
–O5	2.629(2)	Ave.	1.629
–O12	2.674(3)		
–O7	2.736(2)		
–O13	2.914(2)		
Ave.	2.649		

$Na_{1.96}(Sr_{2.91}Ba_{0.03}Ca_{0.03}Pb_{0.02})_{\Sigma 2.99}(Mg_{0.62}Mn_{0.28}Co_{0.07}Fe_{0.01})_{\Sigma 0.98}Si_{6.03}O_{17}$, which can be simplified to $Na_2Sr_3MgSi_6O_{17}$.

The Raman spectrum of meieranite was collected from a randomly oriented crystal with a Thermo Almega microRaman system using a solid-state laser with a frequency of 532 nm at the full power of 150 mW and a thermoelectrically cooled CCD detector. The laser is partially polarized with 4 cm^{-1} resolution and a spot size of 1 μm.

X-ray crystallography

The powder X-ray diffraction data for meieranite were collected with a Rigaku D/Max 2500 diffractometer equipped with Cu$K\alpha$ radiation at 45 KV and 250 mA. Listed in Table 2 are the measured powder X-ray diffraction data, along with those calculated from the determined structure using the program XPOW (Downs *et al*. 1993). The unit-cell parameters obtained from the powder X-ray diffraction data are a = 7.9343(2), b = 10.4741(4), c = 18.2381(5) Å.

Single-crystal X-ray diffraction data were collected from a nearly equidimensional crystal (0.07 × 0.07 × 0.06 mm) using a Bruker X8 APEX2 CCD X-ray diffractometer equipped with graphite-monochromatized Mo$K\alpha$ radiation with frame widths of 0.5° in ω and 30 s counting time per frame. All reflections were indexed on the basis of an orthorhombic unit cell (Table 3). The intensity data were corrected for X-ray absorption using the Bruker program SADABS. The systematic absences of reflections suggested possible space groups $P2_1nb$ (#33) or $Pmnb$ (#62) (non-standard setting to facilitate a direct comparison with the nordite group of minerals; see below). The crystal structure was solved and refined using SHELX2014 (Sheldrick 2015a, 2015b) based on space group $P2_1nb$ because it produced the better refinement statistics in terms of bond lengths and angles, atomic displacement parameters, and R factors. For simplicity, the chemical formula $Na_2Sr_3(Mg_{0.63}Mn_{0.37})Si_6O_{17}$ was adopted during the refinements. In other words, we grouped Mn, Co, and Fe together and treated them as Mn in the refinements. Moreover, all atomic sites were assumed to be fully occupied. The positions of all atoms were refined with anisotropic displacement parameters. An inversion twin was introduced in the refinements, giving rise to a twin ratio of 0.73:0.27. Final coordinates and displacement parameters of atoms in meieranite are listed in Table 4 and selected bond-distances in Table 5. Calculated bond-valence sums using the parameters from Brese & O'Keeffe (1991) are given in Table 6.

Crystal Structure Description and Discussion

The crystal structure of meieranite is characterized by two kinds of layers that alternate along [010] (Fig. 3a): layers of corner-sharing SiO_4 and $M^{2+}O_4$ tetrahedra (M^{2+} = Mg, Mn, Co, Fe) and layers of NaO_6 and SrO_8 polyhedra. The tetrahedral layers

TABLE 6. BOND-VALENCE SUMS FOR MEIERANITE

	Na1	Na2	Sr1	Sr2	Sr3	*M*	Si1	Si2	Si3	Si4	Si5	Si6	Sum
O1			0.211				0.857				0.879		2.020
			0.073										
O2		0.196		0.288			1.150						1.819
				0.185									
O3	0.223		0.337			0.501	1.042						2.103
O4	0.131		0.261				0.916	0.919					2.227
O5			0.266		0.251	0.496		1.007					2.020
O6				0.381	0.326			1.121					1.829
O7					0.188			0.899	0.958				2.046
O8			0.384		0.272				1.126				1.781
O9	0.198	0.107							0.927	0.889			2.124
O10		0.138		0.140					0.920			0.871	2.070
O11		0.221			0.299	0.515				1.041			2.078
O12	0.231	0.216			0.223					1.130			1.799
O13	0.092				0.116					0.850	0.920		1.978
O14				0.377	0.321						1.135		1.834
O15		0.079		0.207							0.879	0.910	2.074
O16	0.152		0.256									1.116	1.738
			0.215										
O17				0.244		0.491						1.072	2.026
				0.219									
Sum	1.028	0.957	2.003	2.042	1.997	2.083	3.964	3.945	3.931	3.910	3.813	3.969	

Note: (1) Parameters for calculations of bond-valence sums were taken from Brese & O'Keeffe (1991).
(2) The bond valence sum for *M* was calculated based on (0.63Mg + 0.37Mn).

consist of four-, five-, and eight-membered rings and are composed of $[Si_6O_{17}]$ ribbons (parallel to [101]) linked together by MO_4 tetrahedra (Figure 4a). According to Chakhmouradian *et al*. (2014), the overall topology of the tetrahedral layer in meieranite can be formulated as $4^15^28^1$, where the normal numbers stand for the membered rings and the superscript numbers for their ratios.

Most remarkably, the crystal structure of meieranite is topologically identical to that of the nordite group of minerals (Figs. 3b and 4b) (Bakakin *et al*. 1970, Pushcharovskii *et al*. 1999). The general chemical formula of the nordite group of minerals can be expressed as $Na_3SrR^{3+}M^{2+}Si_6O_{17}$, where R = Ce and La and M = Zn, Fe, and Mn (Pushcharovskii *et al*. 1999). Accordingly, the chemical composition of meieranite ($Na_2Sr_3M^{2+}Si_6O_{17}$) may be obtained *via* the coupled substitution of $2Sr^{2+}$ for ($Na^+ + R^{3+}$) in nordite. Structurally, it is the Sr2 and Sr3 atoms in meieranite that substitute for ½ Na2 (which has a site multiplicity twice that of Na1) and R^{3+} in ferronordite-(Ce) (Pushcharovskii *et al*. 1999), respectively. Due to the difference in ionic radius and charge between Na^+ and Sr^{2+}, Sr2 and Na2 in meieranite are completely ordered into two distinct sites that are symmetrically equivalent in nordite, resulting in a symmetry reduction from *Pcca* for nordite to $P2_1nb$ for meieranite.

Because the ionic radius of Sr^{2+} (1.26 Å) is greater than that of Na^+ (1.02 Å) or Ce^{3+} (1.143 Å) (Shannon 1976), the coupled substitution of $2Sr^{2+}$ in meieranite for ($Na^+ + R^{3+}$) in nordite not only increases the average bond distances of the corresponding cations (Table 5), but also enlarges the corresponding dimensions of the meieranite structure relative to those of the nordite-type structure. For example, the separation between the two tetrahedral layers increases from 5.19 Å in ferronordite-(Ce) or manganonordite-(Ce) (Pushcharovskii *et al*. 1999) to 5.25 Å in meieranite, whereas the smallest repeatable unit in the $[Si_6O_{17}]$ ribbon direction increases from ~19.85 Å (the *c* dimension) in ferronordite-(Ce) or manganonordite-(Ce) (Pushcharovskii *et al*. 1999) to 19.91 Å (along the [101] direction) in meieranite, suggesting that the $[Si_6O_{17}]$ ribbons in meieranite are less kinked than those in nordites.

Chakhmouradian *et al*. (2014) described the new mineral vladykinite, $Na_3Sr_4(Fe^{2+}Fe^{3+})Si_8O_{24}$, which, as with meieranite and the nordites, also contains tetrahedral layers consisting of four-, five-, and eight-membered rings. However, the topology of its tetrahedral layer is $4^15^48^1$, rather than $4^15^28^1$, as in

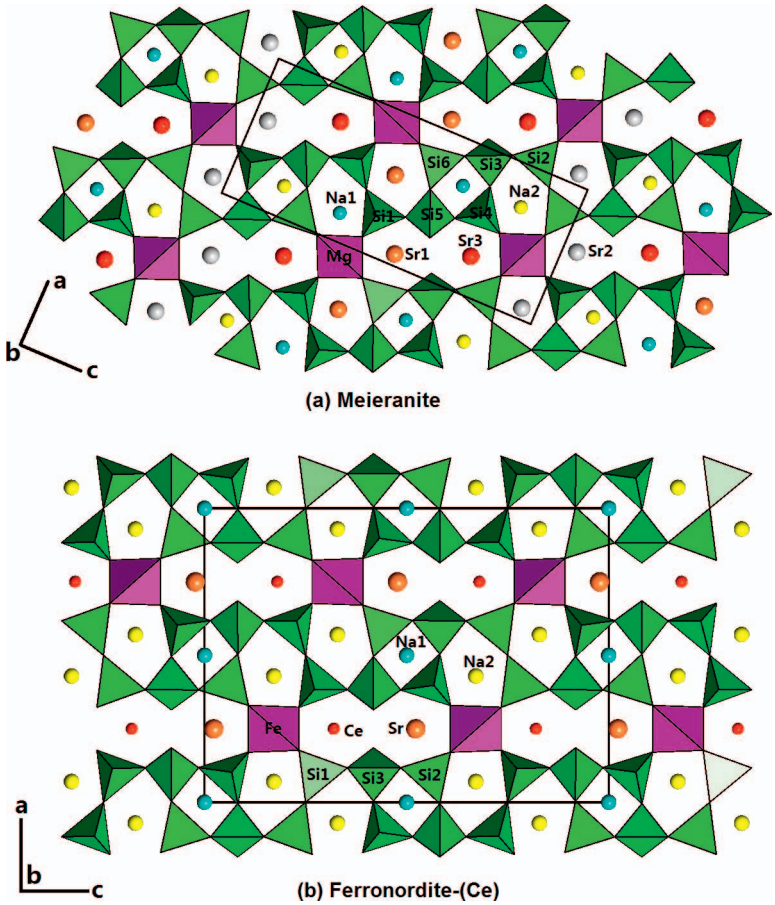

FIG. 4. Crystal structures of (a) meieranite and (b) ferronordite-(Ce), viewed along the **b** axis. All symbols are the same as in Figure 3.

nordites and meieranite. Chakhmouradian *et al*. (2014) further noted that the tetrahedral layer in bussyite-(Ce), $R_2CaNa_6MnBe_5Si_9(O,OH)_{30}(F,OH)_4$ (Grice *et al*. 2009), is topologically identical to that in the nordites and presented an insightful discussion on structural relations among minerals with tetrahedral layers composed of four-, five-, and eight-membered rings, including vladykinite, nordites, bussyite-(Ce), and semenovite-(Ce). Hawthorne *et al*. (2019) thoroughly reviewed the structural hierarchy for minerals containing sheet silicates. Based on their classification, the tetrahedral layer in meieranite, like that in the nordite-type structure, can be considered as a net with three- and four-connected vertices (see Table 6 in Hawthorne *et al*. 2019).

The strong resemblance between the structures of meieranite and the nordite group of minerals is also manifest in their Raman spectra (Fig. 5). Tentative assignments of the major Raman bands for meieranite are as follows: The peaks between 900 and 1200 cm^{-1} are due to Si–O stretching vibrations within the SiO_4 groups. The bands between 750 and 800 cm^{-1} are ascribed to O–Si–O bending vibrations within the SiO_4 groups. The strong bands from 600 to 700 cm^{-1} are attributable to $Si–O_{br}–Si$ bending vibrations between SiO_4 tetrahedra. The weak bands below 600 cm^{-1} are mainly associated with the rotational and translational modes of SiO_4 tetrahedra, as well as the M–O interactions and lattice vibrational modes.

It is interesting to note that M^{2+} is dominated by Mg in meieranite, but by Zn, Fe, or Mn in nordite, ferronordite, or manganonordite, respectively. Because of the structural similarities between meieranite and the nordite-group minerals, we may postulate the existence of Mg-rich nordite and Zn-, Fe-, and Mn-rich

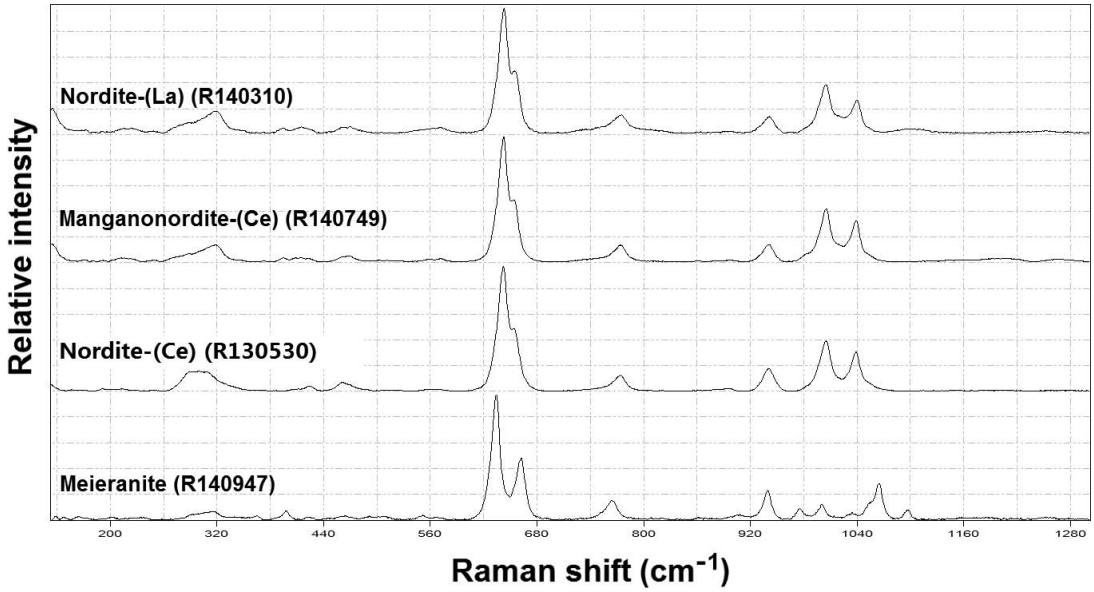

FIG. 5. Raman spectra of meieranite, nordite-(La), nordite-(Ce), and manganonordite-(Ce). The spectra are shown with vertical offsets for clarity.

meieranite. Furthermore, given the coupled substitution of $2Sr^{2+}$ for $(Na^{+} + R^{3+})$ between meieranite and nordite, it is possible that the meieranite-type structure may also be capable of accommodating rare earth elements to some degree.

ACKNOWLEDGMENTS

We are very grateful for the constructive comments by Dr. Henrik Friis, Dr. Sergey Aksenov, and an anonymous reviewer.

REFERENCES CITED

BAKAKIN, V.V., BELOV, N.V., BORISOV, S.V., & SOLOVYEVA, L.P. (1970) The crystal structure of nordite and its relationship to melilite and datolite-gadolinite. *American Mineralogist* **55**, 1167–1181.

BRESE, N.E. & O'KEEFFE, M. (1991) Bond-valence parameters for solids. *Acta Crystallographica* **B47**, 192–197.

CHAKHMOURADIAN, A.R., COOPER, M.A., BALL, N., REGUIR, E.P., MEDICI, L., ABDU, Y.A., & ANTONOV, A.A. (2014) Vladykinite, $Na_3Sr_4(Fe^{2+}Fe^{3+})Si_8O_{24}$: A new complex sheet silicate from peralkaline rocks of the Murun complex, eastern Siberia, Russia. *American Mineralogist* **90**, 235–241.

DOWNS, R.T., BARTELMEHS, K.L., GIBBS, G.V., & BOISEN, M.B., JR. (1993) Interactive software for calculating and displaying X-ray or neutron powder diffractometer patterns of crystalline materials. *American Mineralogist* **78**, 1104–1107.

GRICE, J.D., ROWE, R., POIRIER, G., PRATT, A., & FRANCIS, J. (2009) Bussyite-(Ce), a new beryllium silicate mineral species from Mont Saint-Hilaire, Québec. *Canadian Mineralogist* **47**, 193–204.

GUTZMER, J. & BEUKES, N.J. (1996) Mineral paragenesis of the Kalahari manganese field, South Africa. *Ore Geology Reviews* **11**, 405–428.

HAWTHORNE, F.C., UVAROVA, Y.A., & SOKOLOVA, E. (2019) A structure hierarchy for silicate minerals: sheet silicates. *Mineralogical Magazine* **83(1)**, 3–55.

KLEYENSTUBER, A.S.E. (1984) The mineralogy of the manganese-bearing Hotazel Formation of the Proterozoic Transvaal sequence of Griqualand West, South Africa. *Transactions of Geological Society of South Africa* **87**, 267–275.

MANDARINO, J.A. (1981) The Gladstone-Dale relationship: Part IV. The compatibility concept and its application. *Canadian Mineralogist* **19**, 441–450.

PUSHCHAROVSKII, D.Y., PEKOV, I.V., PLUTH, J.J., SMITH, J., FERRARIS, G., VINOGRADOVA, S.A., ARAKCHEEVA, A.V., SOBOLEVA, S.V., & SEMENOV, E.I. (1999) Raite, manganonordite-(Ce), and ferronordite-(Ce) from the Lovozero massif: Crystal structures and mineralogical geochemistry. *Crystallography Reports* **44**, 565–574.

SHANNON, R.D. (1976) Revised effective ionic radii and systematic studies of interatomic distances in halides and chalcogenides. *Acta Crystallographica* **A32**, 751–767.

SHELDRICK, G.M. (2015a) *SHELXT* – Integrated space-group and crystal structure determination. *Acta Crystallographica* **A71**, 3–8.

SHELDRICK, G.M. (2015b) Crystal structure refinement with *SHELX*. *Acta Crystallographica* **C71**, 3–8.

VON BEZING, K.L., DIXON, R.D., POHL, D., & CAVALLO, G. (1991) The Kalahari Manganese Field, an update. *Mineralogical Record* **22**, 279–297.

Received November 20, 2018. Revised manuscript accepted March 26, 2019.